# Low-Power Wide Area Network Technologies for Internet-of-Things: A Comparative Review

Augustine Ikpehai, *Member, IEEE*, Bamidele Adebisi, *Senior Member, IEEE*, Khaled M. Rabie, *Member, IEEE*, Kelvin Anoh, *Member, IEEE*, Ruth E. Ande, *Graduate Student Member, IEEE*, Mohammad Hammoudeh, *Member, IEEE*, Haris Gacanin, *Senior Member, IEEE*, and Uche M. Mbanaso, *Member, IEEE*

***Abstract*—The rapid growth of Internet-of-Things (IoT) in the current decade has led to the development of a multitude of new access technologies targeted at low-power, wide area networks (LP-WANs). However, this has also created another challenge pertaining to technology selection. This paper reviews the performance of LP-WAN technologies for IoT, including design choices and their implications. We consider Sigfox, LoRaWAN, WavIoT, random phase multiple access (RPMA), narrowband IoT (NB-IoT), as well as LTE-M and assess their performance in terms of signal propagation, coverage and energy conservation. The comparative analyses presented in this paper are based on available data sheets and simulation results. A sensitivity analysis is also conducted to evaluate network performance in response to variations in system design parameters. Results show that each of RPMA, NB-IoT, and LTE-M incurs at least 9 dB additional path loss relative to Sigfox and LoRaWAN. This paper further reveals that with a 10% improvement in receiver sensitivity, NB-IoT 882 MHz and LoRaWAN can increase coverage by up to 398% and 142%, respectively, without adverse effects on the energy requirements. Finally, extreme weather conditions can significantly reduce the active network life of LP-WANs. In particular, the results indicate that operating an IoT device in a temperature of −20 °C can shorten its life by about half; 53% (WavIoT, LoRaWAN, Sigfox, NB-IoT, and RPMA) and 48% in LTE-M compared with environmental temperature of 40 °C.**

***Index Terms*—Access technologies, energy conservation, Internet-of-Things (IoT), link budget, LoRaWAN, low-power wide area network (LP-WAN), LTE-M, narrowband IoT (NB-IoT), random phase multiple access (RPMA), sensitivity analysis, Sigfox, WavIoT.**

## I. Introduction

By 2025, up to 75 billion devices would be connected in Internet-of-Things (IoT), with potential economic impact of around $11.1 trillion a year [1], [2]. The key underpinning of IoT is the large number of interconnected devices that exchange information and enable services. Although IoT connectivity will be dominated by short-range technologies for many years, the work [3] predicts that by 2025, 25% of wireless industrial IoT connections will be provided with low-power, wide area network (LP-WAN) technologies including LoRa,[1] Sigfox, LTE-M, as well as narrowband IoT (NB-IoT). This signifies the continued importance of LP-WAN as the IoT landscape evolves.

Machine-to-machine communication in IoT represents a very large market, growing rapidly at compound annual growth rate of over 20% [5]. Nevertheless, the market is fragmented and awash with many access technologies and vertical solutions that sometimes do not interoperate. The result is that despite the potentials of IoT, organizations, and end users are faced with overwhelming choices of access technologies. Therefore, it becomes challenging to decide, where or how to begin their IoT road map as part of their wider digital transformation journey. Insufficient comparative studies of LPWAN technologies has been identified as one of the major barriers to potential IoT users [6]. This paper does not involve detailed physical or media access control (MAC) layer specifications, the results nevertheless provide indicative performance of the LP-WAN technologies set-up under the same operating conditions.

Until now, most of the studies independently evaluated LP-WAN technologies in different operating environments. The main reason is that many of the leading technologies are based on proprietary protocols whose detailed specifications are not freely available in the public domain. For example, LoRaWAN and Sigfox are the top two LP-WAN technologies in terms of installed base. The underlying chirp spread spectrum (CSS) modulation technique in the physical layer of LoRa is proprietary and owned by Semtech Corporation. On the other hand, Sigfox deploys and operates the network but freely provides the protocol specification to

Manuscript received June 28, 2018; revised September 5, 2018 and October 31, 2018; accepted November 20, 2018. Date of publication November 28, 2018; date of current version May 8, 2019. This work was supported in part by the CityVerve: IoTs and Smart Cities Demonstrator project through Innovate U.K., under Grant 102561 and in part by the Triangulum (Part of H2020 Smart Cities and Communities Programme) through the European Commission under Grant 646578-Triangulum-H2020-2014-2015/H2020-SCC-2014. *(Corresponding author: Augustine Ikpehai.)*

A. Ikpehai, B. Adebisi, K. M. Rabie, K. Anoh, R. E. Ande, and M. Hammoudeh are with the Faculty of Science and Engineering, Manchester Metropolitan University, Manchester M1 5GD, U.K. (e-mail: a.ikpehai@mmu.ac.uk; b.adebisi@mmu.ac.uk; k.rabie@mmu.ac.uk; k.anoh@mmu.ac.uk; ruth.e.ande@stu.mmu.ac.uk; m.hammoudeh @mmu.ac.uk).

H. Gacanin is with the Department of Artificial Intelligence Communication Systems, Indoor Networks, Access Lab, Nokia Bell Labs, 2018 Antwerp, Belgium (e-mail: haris.gacanin@nokia-bell-labs.com).

U. M. Mbanaso is with the Centre for Cyberspace Studies, Nasarawa University, Keffi PMB 1029, Nigeria (e-mail: uche.magnus@mbanaso.org).

Digital Object Identifier 10.1109/JIOT.2018.2883728

[1]In this paper, LoRa denotes the physical layer modulation only, while LoRaWAN refers to the wide area network protocol suite that adopts LoRa at physical layer and LoRa MAC at media access control sublayer [4].

chips manufacturers. Thus, LoRa is a closed chipset but open network; (even private networks are possible) and Sigfox is a closed network but open chipset. The implication is that in the former, Semtech controls the production, support and price of LoRa chipsets, while in the latter, Sigfox controls the provision, access and price of the network resources. Other technologies are different variants of either proprietary physical or MAC layer. Hence, no mainstream LP-WAN protocol stack is currently fully open.

However, given the scope of IoT, it is important for solution providers, system designers and users to have a wide perspective of LP-WAN options without being locked-in. Motivated by that gap, the objective of this paper is to assess the performance of the widely available LP-WAN technology specifications. The system parameters used are mostly drawn from the datasheets of the respective device manufacturers.

The contribution of this paper is twofold. First, we identify an approach to optimize the LP-WAN by exploiting the link budget and design parameters without increasing the energy requirements of the system. The second contribution resides in identifying the multivariate dependence of energy consumption on field, application and technology-specific characteristics, each of which can be exploited to different extents. These results provide useful insights which are extremely valuable when deciding the tradeoff between network performance, design complexity and cost.

## II. Related Work

LP-WAN technologies are increasingly being deployed as last mile connectivity to compliment traditional technologies and replace them in many use-cases. However, majority of existing studies that compare the LP-WAN technologies are either literature reviews [7]–[11] or brief experiments with two or three technologies and are often focused on a single aspect of the systems. The studies neither include rigorous analysis of multiple performance metrics nor investigate how the technologies perform relative to each other in different environments, using identical system parameters. In some evaluation cases, the technologies were tested in one environment and are therefore limited in scope.

In many of the studies, where practical systems were designed, comparisons were not made with competing LP-WAN solutions. In fact, in some of the experiments, single technology was deployed for particular use-case which also limits the assessment outcomes to type-specific scenarios [12], [13]. In some other works, the comparisons were restricted to physical and associated MAC layers only while some evaluation studies focused on either cellular-only or noncellular LP-WAN technologies [5], [14], [15]. However, as some of the LP-WAN technologies are still at their infancy, many practical issues are being resolved. Thus, a cross-cutting comparison will not only identify suitability for specific applications but also ascertain among the LP-WAN specifications, the extent of design diversity in relation to the network performance.

LoRaWAN is currently one of the most deployed LP-WAN access networks for IoT [16] and also one of the widely reported LP-WAN technologies in literature. Signal propagation is crucial in IoT [17] as it affects network performance in terms of coverage, reliability, and data rate. Path loss and coverage have been reported in many LP-WAN studies including LoRa [18] and NB-IoT [19] while [20] proposed an indoor channel attenuation model for LoRa, following a series of measurement campaigns. A few other empirical studies, such as [21] compared the performance of LoRa's CSS modulation scheme with frequency-shift keying. This paper found that coverage and network reliability are both affected by the payload size. However, the experiments were limited to the university environment and the results did not provide insights into potential behaviors in other environments. More challenging terrains, such as dense urban areas and other metropolitan environments with higher levels of interference may exhibit different performance due to difference in the interference sources and patterns. This will not only provide additional insights but also help to analyze the results in the context of individual field environment.

For cellular LP-WANs, [22] investigated the capacity and coverage of LTE-M and NB-IoT in a rural area in Denmark. This paper reported that cellular technologies, such as LTE-M support maximum coupling loss of about 156 dB, however, in deep indoor applications can experience up to additional 30 dB penetration loss. An interesting aspect would be a comparison with noncellular technologies.

Apart from the various analytical models that have been reported [23]–[25], other experimental studies have been conducted to individually evaluate different aspects of LP-WAN including coverage [26], [27], energy consumption [28], capacity [22], [29], [30], and scalability [23], [24], [30]. The main commonality in these and many other existing studies is that they mostly focused on one or two technologies. Comparing results from different studies may not provide a balanced view as each experiment or simulation model is conducted with a set of assumptions or conditions which varies across studies and authors.

According to [31], until recently, there were very few studies involving more than three technologies. Although, [31] compared the performance of GPRS and NB-IoT with Sigfox and LoRa, the dearth of publications in this area suggests that a considerable amount of follow-on work still needs to be carried out. The objective of this paper is therefore to contribute in that regard.

Recent reviews of LP-WANS are summarized in Table I according to their areas of focus. Many of them describe single technologies while energy consumption was not considered in most. However, given its importance in IoT generally and LP-WANs in particular, it is necessary to consider the energy performance of existing LP-WAN technologies as part of a complete system review.

## III. Link Budget and Implications in LP-WANs

LP-WANs in IoT access networks share similar implementation methodologies with traditional wireless networks but with some differences in system design. According to Shannon–Hartley theorem, the signal-to-noise ratio (SNR) of each bit can be written as [38]

$$\frac{E_b}{N} = \frac{\varepsilon}{C}\left(2^{\frac{C}{\varepsilon}} - 1\right) = \frac{2^{\eta} - 1}{\eta} \tag{1}$$

TABLE I
SUMMARY OF RELATED WORK

| Ref. | Specification | Focus area | Contribution/ Methodology | Energy? | Limitations/Gaps |
|---|---|---|---|---|---|
| [7], [32] WavIoT | LoRa & Sigfox, RPMA or | bands. Description of advantages | Basic literature review & grouping into licensed and unlicensed of LP-WANS over legacy long range technologies. | No performance | Little analytic rigour. No comparison or evaluation. |
| [8] | LoRaWAN | Basic overview & discussion of LP-WAN technologies. | Description of LoRaWAN in terms of capacity, security, battery life. | Yes | Only LoRaWAN studied. Other cellular and non-cellular LP-WANs excluded. |
| [33] | LTE-M, NB-IoT, LoRa, Sigfox, RPMA. | | Description of each technology and measurements of reliability. | No | Insufficient depth of review. No performance comparison or evaluation. |
| [5], [9], [11] | Sigfox, LoRa, NB-IoT, 3G/4G | | Very basic comparison of technologies & their differences. | | |
| [27] | 5G | | Indoor coverage evaluation based on ray tracing. | No | Only 1 site & 1 technology considered. |
| [34] | 5G, LTE-M, EC-GSM | | Description of various cellular , LP-WANs enablers & applications. | No | Comparative performance with non-cellular LP-WANs was not considered. |
| [16], [30] | LoRaWAN | Comprehensive review or tutorial | Capacity, scalability, densification, use-cases and reliability. Used simulation to illustrate the limits of LoRaWAN: scalability & reliability. | No | Battery life and its dependencies were not covered. LoRaWAN not compared with other LP-WANs. |
| [35] | NB-IoT | | Comprehensive review of NB-IoT including security, applications & energy consumption | Yes | NB-IoT not compared with other technologies |
| [13] | LoRa/LoRaWAN | Experimentation, evaluation, system design & implementation. | Deployment of LoRa to monitor a river. Measurements taken. | No | Only LoRa considered. One use-case studied. |
| [17] | | | Indoor signal propagation characteristics using RSSI as measure of performance. | No | Only LoRa studied. Performance relative to other technologies were not reported. |
| [20] | | | Measurement-based attenuation model: coverage and reliability for land and sea | No | |
| [36] | | | Indoor evaluation: SNR, packet loss, throughput RSSI, energy consumption. | Yes | |
| [37] | | | Effects of interference on scalability. Evaluation of LoRa in terms of coverage, reliability using CSS & FSK in terrestrial deployments. | No | Single technology considered. |
| [21] | | | | No | |
| [28] | NB-IoT | | Experimental evaluation of energy consumption of NB-IoT devices. | Yes | Only NB-IoT studied Performance relative to other other technologies were not reported. |
| [14] | | | NB-IoT firmware developed & deployed on devices. Cloud platform, application server, user application also deployed. | No | |
| [18], [23] | LoRa | Simulation or analytical solution for LP-WANs | Simulation of LoRa with multiple SF and rates. Distribution of SF and discrete power settings to reduce packet rerror rate (PER). | Yes | Only LoRa investigated. Performance relative to other technologies not reported. |
| [29] | | | Detailed analysis of LoRa and LoRaWAN, simulation of throughput & collision rate and measurements of coverage & reliability. | No | |
| [19] | NB-IoT | | Coverage of NB-IoT based on in-band deployment in LTE. | No | Only NB-IoT investigated. |
| [22] | LTE-M, NB-IoT | | Coverage, reliability, energy consumption in indoor and outdoor cases. | Yes | Non-cellular LP-WANs not covered |
| [24] | Sigfox | | Derivation of expression of packet error rate for UNB LP-WAN such as Sigfox. | No | Only Sigfox investigated. |
| [25] | LoRa, NB-IoT Sigfox | | Description of MAC of LoRa, NB-IoT & Sigfox. Comparison of PER. | No | Energy & its dependencies were excluded. |

where $C$ is the capacity (in bits/s), $\varepsilon$ is the bandwidth, and $\eta$ is the spectral efficiency (in bits/s/Hz). For a bit duration of $(1/C)$ s, if $S$ denotes the average signal power of each bit and $N$ the noise power in Watts, the average energy per bit is $E_b = (S/C)$ (in J) and the total noise power is $N \cdot \varepsilon$ Watts. The implication of (1) is that, $(E_b/N)$ varies with $\eta$ and the modulation scheme in LP-WAN technologies must ensure that $\eta$ is maximized. For a wireless signal to be correctly decoded

TABLE II
LINK BUDGET OF LP-WAN TECHNOLOGIES USED IN THE SIMULATION [4], [31], [47]–[52]

| Technology | NB-Fi (WavIoT) | LoRaWAN | U-NB(Sigfox) | RPMA (Ingenu) | LTE-M | NB-IoT |
|---|---|---|---|---|---|---|
| | 868MHz | 868MHz | 868MHz | 2.4GHz | 1.8-2.7GHz | 700-2100 MHz |
| Downlink | DL | DL | DL | DL | DL(2.6GHz) | DL(882MHz,1840MHz) |
| Tx Power, dBm | 30 | 21 | 24 | 21 | 40 | 35 |
| Tx cable loss,dB | -3 | -3 | -6 | -3 | -3 | -3 |
| Bandwidth (kHz) | 0.1 | 125 | 0.1/0.6 | 1000 | 1400 | 180 |
| Tx antenna gain, dBi | 0 | 9 | 9 | 9 | 10 | 16 |
| $\sigma$, dBm | -147 | -137 | -129 | -133 | -129 | -141 |
| Rx env. noise | 0 | 0 | 0 | 0 | 0 | 0 |
| Rx antenna gain | 0 | 0 | 0 | 8 | 0 | 0 |
| **Total (link budget)** | **174** | **164** | **156** | **168** | **176** | **189** |
| Obstacle loss (fixed), dB | 20 | 20 | 20 | 30 | 30 | 30 |
| Obstacle loss (variable), dB | 35.8 | 28.1 | 30.7 | 29.8 | 27.1 | 29.4 |

at the receiver, it must meet energy detection threshold. The receiver sensitivity ($\sigma$) can be expressed as [39]

$$\sigma = \frac{E_b}{N} + 10 \cdot \log_{10} C + (\phi - 174\,\text{dBm}). \tag{2}$$

The noise figure ($\phi$) is typically around 2 to 6 dB for LP-WAN radio front-end [39], [40].

In many access networks, such as Sigfox and LoRaWAN, each message sent by the end node can be received by multiple gateways. According to [41]–[43], the potential throughput available per coverage unit can be expressed as

$$R(\lambda, \theta) = \lambda \cdot \log_2(1+\theta)\text{Pr}(\text{SNR} \geq \theta) \tag{3}$$

where $\lambda$ is the gateway density, Pr(.) is the probability operator, $\theta$ is the threshold SNR and $R$ is the potential throughput in bps/Hz/km$^2$. However, (3) assumes fixed data rate and does not provide rate adaptation such that the bit rate of a gateway is adjusted upward or downward according to the SNR instead of outage when the receiver SNR $< \theta$. On the other hand, the average area spectral efficiency (ASE) also in bps/Hz/km$^2$ considers SNR of individual gateway and avoids outage at low SNR by reducing the data rate instead, this is more amenable to IoT scenarios. The ASE can be expressed as [44]

$$\mathscr{E}(\lambda) = \lambda \cdot \mathbb{E}\big[\log_2(1+\text{SNR})\big], \ \text{SNR} \geq \theta. \tag{4}$$

Equation (4) supports bit rate adaptation according to the SNR instead of outage. According to [41]–[44], ASE depends on the number of gateway per km$^2$ and path loss. The value of $\sigma$ can also be reduced to extend the transmission range, however, the performance penalty is reduced bit rate which is acceptable in many IoT deployment scenarios. This systematic tradeoff underpins the long range operation of LP-WAN technologies. The value of $\sigma$ in LP-WANs is typically lower than $-128$ dBm ($-129$ dBm to $-155$ dBm) and ranges from $-90$ dBm to $-110$ dBm [45] in traditional wireless systems, such as Wi-Fi [46]. The implication is that in terms of absolute signal power in Watts, LP-WAN receivers can detect wireless signals that are 1000 times weaker than Wi-Fi and other technologies with $-100$ dBm sensitivity. LP-WAN technologies exploits this capability in the various specifications.

Table II presents the technical specifications of widely available LP-WAN technologies from datasheets [4], [47], [48], measured obstacle losses in European urban environments [48] as well as other parameters reported in [31] and [49]–[52]. It

TABLE III
ADDITIONAL SIMULATION PARAMETERS

| Parameter | Value |
|---|---|
| Number of gateways | 1 |
| Baseline payload | 12 bytes |
| Radio electronics energy,$E_{elec}$ | 50 nJ/bit |
| On-Air time | Sigfox-EU:6.24s<br>LoRa (varies with SF) |
| Background noise, dBm | -130 dBm |
| Battery model | E91-AA alkaline battery |

is generally desirable that the main lobe of the transmitted radiation pattern reaches the receiver to ensure that maximum signal strength and coverage are delivered. The field condition can be worsened by obstruction losses which will further reduce the link budget. The fixed obstacle losses in Table II are the reported average values obtained from measurements in urban areas in Europe through 20 cm concrete walls [48].

The parameters in Tables II and III are used to simulate the transmission from gateway to end device based on the scenario described in the next section. Sigfox and LoRa are two leading LP-WAN technologies. However, Sigfox supports a maximum payload of 12 bytes while LoRa can support up to 242 bytes [36], [53], [54]. In order to compare the technologies, we adopt Sigfox payload as the baseline in Table III. Energy consumed by the radio electronic circuit in low-power devices, such as wireless sensors has been reported to be about 50 nJ/bit [55], [56]. The choice of Alkaline battery is informed by the fact that they are low-cost, widely available, and are commonly used in low-power applications, such as wireless sensor networks. In Europe, at 100 kb/s, it takes about 2.08 s [57] to send a 12-byte Sigfox frame and since the endpoints do not synchronize with Sigfox base station, each message is sent three times to improve chances of detection [5], [58].

## IV. NETWORK MODEL AND METHODOLOGY

This paper considers an access network in which the gateway antenna is at 25 m height on a tower and the IoT end point comprises an antenna located at 8 m (based on the average height of 2-story building in U.K. [21], [59]). This set-up applies to many IoT and smart city scenarios including monitoring of multistory building packing space availability in smart cities, monitoring of structural health of buildings

and bridges, detection of noise map in urban areas, smart grid, industrial IoT, etc. The downlink is considered and we discuss the network performance in different terrains including open/rural areas, suburban, small and large cities. In each case, the indicative performance of the network is analyzed following simulation of each access technology in different environments. In this paper, EU-868 LoRaWAN/Sigfox, WavIoT, 2.4 GHz RPMA-Ingenu, 2.6 GHz LTE-M, NB-IoT (882 MHz/1840 MHz) specifications and other parameters outlined in Table II are employed in the simulation using MATLAB. The 3GPP recommends in-band deployment for LTE-M using existing LTE installed base. In this paper, we adopt the 2.6 GHz for LTE-M as it is widely used in Europe and beyond in existing LTE systems.

Although NB-IoT supports three modes of deployment, namely; standalone, in-band LTE, and guard band in LTE, it can also coexists with GSM, LTE, and UMTS [60]. We adopt 882 and 1840 MHz for NB-IoT which are equivalent to bands 5 and 3 downlink frequencies, respectively, in 3GPP NB-IoT (release 13) [49]. These choices are informed by the fact that many mobile operators already own blocks of frequency in 1800 MHz band and 800–900 MHz used for various services, such as GSM and LTE. This clearly provides an upgrade path to NB-IoT for such operators through frequency refarming.

In IoT access network design and implementation, the three most critical questions are as follows.

1) What is the maximum distance the link can cover without compromising quality-of-service or SNR.
2) What field parameters can be explored to reduce cost of implementation.
3) What endogenous variables can be tweaked to conserve energy [61] and optimize network performance.

To address these questions, the methodology adopted is summarized as follows.

1) Use of system-specific attributes of WavIoT, Sigfox, LoRaWAN, random phase multiple access (RPMA), and LTE-M to generate propagation characteristics including Fresnel clearance and path loss.
2) Application of equal transmit power across the technologies, followed by estimation of the corresponding coverage at each power level in rural and urban environments.
3) For each technology, the path loss information previously calculated is extracted and used to generate the received signal strength indicator (RSSI) as well as SNR at different distances in the field. SNR is benchmarked against 20 dB widely used in conventional wireless systems.
4) As coverage is more challenging in urban areas, a sensitivity analysis is conducted for urban deployment scenario with a view to exploiting system parameters for network performance optimization.
5) Investigation of the key factors affecting energy consumption in end devices.
6) For specific LP-WAN system configurations, estimate the battery life of the radio transceiver based on 1% maximum duty cycle allowed in Europe.

While there are no simple or direct answers to the questions posed, the following sections illustrate these issues and provides insights to different aspects of the questions with some rationales.

## V. Signal Propagation

### A. Fresnel Clearance

Ideally, radio waves should travel in a straight line from the source to destination. An obstruction that is close to or infringing the LoS causes attenuation. For the given scenario, the Fresnel clearance is illustrated in Fig. 1.

The Fresnel zone radius at a point $P$ along the LoS is generally defined as [62]

$$F_{zr} = \sqrt{\frac{n \cdot cd_1 d_2}{f \cdot D}} = 17.32\sqrt{\frac{d_1 d_2}{f \cdot D}} \tag{5}$$

where $n = 1$ denotes the first Fresnel zone, $c$ is the speed of light, $f$ is the frequency in GHz, and $D = d_1 + d_2$ is the total distance in km. In reality, at least 60% Fresnel clearance is required.

By applying (5), Fig. 2 presents the minimum clearance requirements for 868 MHz, 2.4 GHz, and 2.6 GHz LP-WAN technologies as the obstacle is moved to different points along the transmission path in a 50 km network. It can be seen that the required Fresnel clearance increases as the obstacle moves toward the midpoint such that the largest clearance is required if the obstacle is positioned at the middle. Fig. 2 further shows that when the obstacle is moved from 1 to 5 km then 25 km, with LTE-M, the minimum clearance increases from 6.38 to 13.67 m then 22.79 m, respectively. In the Sigfox/LoRaWAN networks with the obstacles at the same positions, the minimum Fresnel clearance are, respectively, 11.04, 23.66, and 39.44 m. The key observation here is that the closer the obstruction to the gateway transmitter, the more impact it has on the access network.

### B. Path Loss

Path loss estimation is a crucial part of planning and design of the access networks. In wireless communication, every time the distance is doubled, only one-fourth of the signal power is received and this has some far-reaching implications for connectivity in IoT as it degrades the SNR at the end receiver. The path loss discussed in this paper relates only to outdoor applications. The free space path loss (FSPL) model is based on clear LoS and does not take into account terrestrial objects, such as hills, trees, buildings, etc. In ideal case, the path loss experienced by signals can be expressed as

$$\text{FSPL(dB)} = 20 \cdot \log_{10} l + 20 \cdot \log_{10} f - 32.44 \tag{6}$$

where $l$ is the distance (in km) and $f$ is the frequency (in Hz). However, the assumption of free space between the transmitter and receiver in FSPL is invalid in many real life deployments, as radio frequency (RF) paths are typically laden with additional factors which further degrade the path loss. Such factors include [63] cable losses, antenna gain, LoS condition, receiver

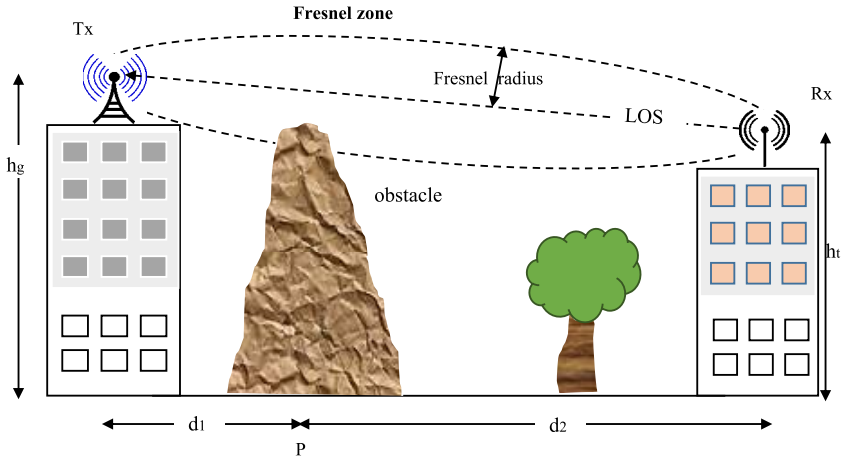


Fig. 1. LoS condition and Fresnel clearance.

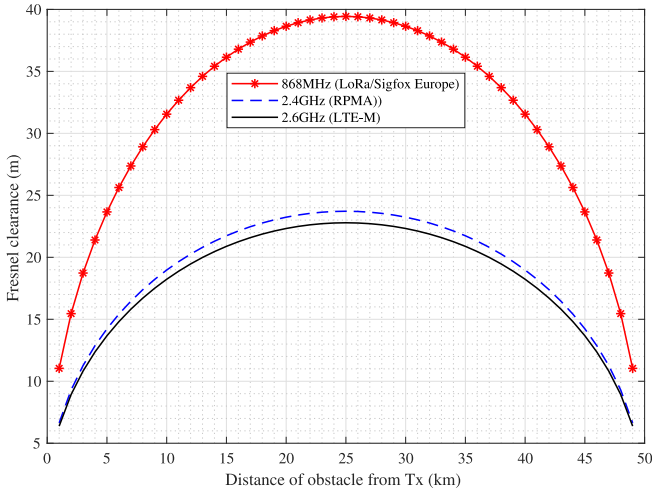


Fig. 2. Effects of obstacle position on Fresnel clearance.

TABLE IV
EXAMPLES OF MATERIALS AND SIGNAL ATTENUATION AT 2.4 GHz [63], [64]

| Material/object | Attenuation | Frequency |
|---|---|---|
| Dry wall | 3dB | 2.4GHz |
| Glass wall with metal frame | 6dB | 2.4GHz |
| Office window | 3dB | 2.4GHz |
| Metal door (non-solid) | 6dB | 2.4GHz |
| Wood | 3dB | 2.4GHz |
| Solid concrete (e.g. wall, bridge) | 8-15dB | 2.4GHz/1.3GHz |
| Aluminum siding | 20.4dB | 815MHz |
| Concrete floor | 10dB | 1.3GHz |
| 6-inch diameter metal pole | 3dB | 1.3GHz |

sensitivity, etc. Particularly in IoT, a wireless signal will typically encounter different obstacles on its path and each has an additive effect on the total path loss. Common examples of obstacles and their attenuation factors are summarized in Table IV.

According to Table IV, if Sigfox or LoRaWAN signal with transmit power of 14 dBm encounters a nonsolid metal door on its path, the signal power is reduced to 8 dBm (approximately 25% of its original value) when it exits the door. In urban areas with high vehicular density and high-rise buildings, signal can suffer from reflection from metallic surfaces, diffraction or even scattering off the lampposts and moving vehicles which contribute to the overall losses. If multiple copies of the signal arrive the receiver, they can destructively interfere and severely degrade reception. The path loss can be expressed as

$$\sigma = P_t + \text{Gain}_{\text{net}} - \text{PL} \tag{7}$$

where $\sigma$ is the receiver sensitivity, PL is total the path loss in dB and $\text{Gain}_{\text{net}}$ is the net gain. The $G_{\text{net}}$ includes all gains resulting from transmit and receive antenna as well as all losses related to the radio and antenna hardware including filters, cables, attenuators, antennas, and obstacle losses, etc. The $\sigma$ in (7) is equivalent to the minimum signal power that will be detected by the receiver. The IoT implementation engineer must therefore ensure that the received power is often greater than $\sigma$.

*1) LP-WAN and Signal Propagation in Different Terrains:* From (7), it is clear that adequate knowledge of the terrain is required in the network design. Some models derived from empirical studies have been reported to provide more realistic path loss. In particular, the Hata–Okumura model, which is based on various Okumura correction functions is widely used for predicting path loss in RF planning in the wireless communication industry. The key strength of this model is that it caters for different field scenarios, such as large cities, small suburban and rural environments [65]–[68] which has influenced its wide acceptance. In its general form, the model can be expressed as

$$\begin{aligned}\text{PL}_{\text{Hata}} = {} & 69.55 + 26.16 \cdot \log_{10} f - 13.82 \cdot \log_{10} h_g \\ & - a(h_t) + \left[44.9 - 6.55 \cdot \log_{10} h_g\right] \log_{10} d - c_t\end{aligned} \tag{8}$$

where $f$ is the frequency (in MHz), $h_g$ is the gateway antenna height (in m) and $d$ is the distance (in km) from transmitting to receiving antenna. The terrain parameter $a(h_t)$ is a function of IoT terminal height, defined for urban areas as

$$a(h_t)_{(\text{urban})} = 3.20\left[\log_{10}(11.75h_t)\right]^2 - 4.97 \tag{9}$$

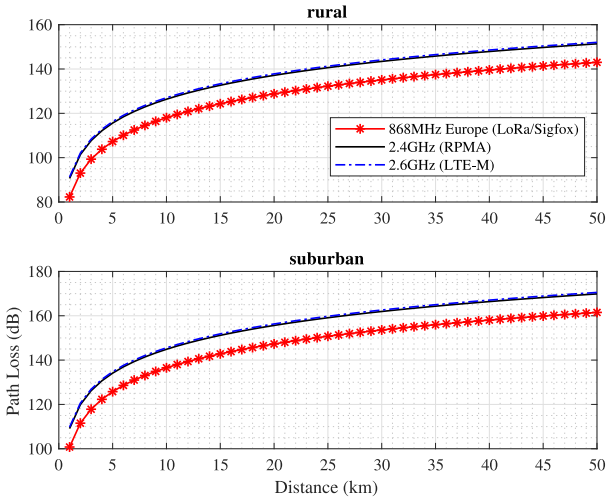


Fig. 3. Path loss of access technologies in rural and suburban environments.

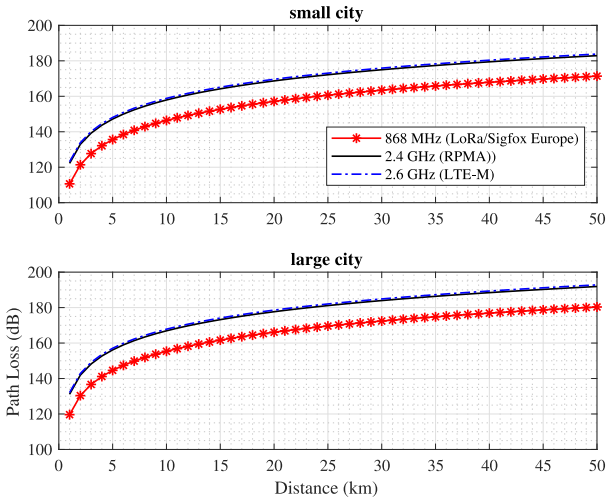


Fig. 4. Path loss of access technologies in urban environments.

for suburban, open and rural areas, $a(h_t)$ is defined as

$$a(h_t)_{(\text{sub}-\text{rural})} = \left[1.1 \cdot \log_{10} f - 0.7\right] h_t - \left[1.56 \cdot \log_{10} f - 0.8\right] \tag{10}$$

where $h_t$ is the height of the remote terminal (IoT endpoint) antenna above the ground. Also, the parameter $c_t$ is the correction factor defined as

$$c_t = \begin{cases} 4.78 \cdot \left[\log_{10} f\right]^2 - 18.33 \cdot \log_{10} f + 40.94, & \text{rural/open} \\ 2\left[\log_{10}\left(\frac{f}{28}\right)\right]^2 + 5.4, & \text{suburban} \\ 0, & \text{urban.} \end{cases} \tag{11}$$

For the various access technologies, the path loss in different environments is presented in Figs. 3 and 4.

By applying (8)–(11) using the parameters in Tables II and III, Figs. 3 and 4, respectively, illustrates the path loss in urban and rural environments for the scenario presented in Fig. 1. These results generally agree with the literature, for instance Fig. 3(a) closely aligns with the coupling loss of 156 dB reported in [22] for LTE-M. It can be seen in Fig. 3 that at a distance of 3 km between the transmitter and receiver, RPMA and LTE-M each incurs additional path loss of about 9 and 11 dB in rural and large cities, respectively, relative to Sigfox/LoRaWAN. At 10 km, the additional path loss experienced by RPMA and LTE-M are 8.2 and 9.2 dB in rural areas as well as 12 and 13 dB, respectively, in large cities (compared with Sigfox/LoRaWAN). These results are within the range of those in [6] and [27] which reported that LP-WAN could achieve up to 20 dB improvement over cellular systems. It is also noted that RPMA and LTE-M are more susceptible to path loss than LoRaWAN and Sigfox. The amount of loss also depends on the nature of the obstacle (Table III), the results in this section, however, show that as the frequency increases, the ability to overcome obstacles drastically reduces. The 868 MHz technologies require significantly taller masts or towers. If that is considered against the fact that attenuation is more pronounced in the >2 GHz region and many ISM radio equipment (e.g., Wi-Fi and ZigBee) also share the 2.4 GHz band, then the system designers and implementation engineers need to consider the delicate balance between network reliability, cost, and efficiency in the choice of radio technology. Although more bandwidth is available in 2.4 and 2.6 GHz compared to 868 MHz, however, Figs. 3 and 4 show that at every distance, the 2.x GHz technologies (RPMA, LTE-M) incur at least 9 dB additional path loss which suggests that they are less able to overcome the effects of obstacles.

*2) Non LoS Propagation:* For IoT applications in urban environments lined with high rise buildings and tall street furniture, non LoS (NLOS) links arise when the gateways and IoT end points are located on two parallel or intersecting streets. With a rectangular street grid, signals experience reflection off the walls as well as diffraction at the building corners [69] and other vertical structures, such as lamp posts and bus stop signage, located near the street junction or parallel street. In such cases, the arriving signals undergo multiple reflections from the walls on the main and side streets as well as scattering around the vertical objects. The 1-turn path loss, relative to free space can be expressed as [70]

$$\text{PL}_{1-\text{Turn}} = \text{PL}_{\text{LOS}} \cdot \frac{\cos^2 \varphi}{S^2} \cdot \frac{x_1 x_2}{x_1 + x_2} \tag{12}$$

where $x_1$, $x_2$ are the distances from the intersection to gateway and end device, respectively, $S$ is the scattering parameter and $\varphi$ is the viewing angle from the gateway to end device which depends on the heights of the antennas. The $\text{PL}_{\text{LOS}}$ term in (12) is the ITU-LOS path loss model defined as

$$\text{PL}_{\text{LOS}} = \begin{cases} 10^{\delta_{\text{dB}}/10}\left(\frac{\gamma^2}{8\pi . h_g . h_t}\right)^2 \left(\frac{d}{d_c}\right)^{2.5}, & d \le d_c \\ 10^{\delta_{\text{dB}}/10}\left(\frac{\gamma^2}{8\pi . h_g . h_t}\right)^2 \left(\frac{d}{d_c}\right)^{4}, & d > d_c \end{cases} \tag{13}$$

where $\delta$ is the environmental parameter, $d$ is the total distance $x_1 + x_2$, and $d_c$ is the cross-over distance. In general, $\text{PL}_{\text{LOS}}$ will vary across different environments, depending on building heights, antenna height, and the amount of waveguide provided by the street canyon. By employing a virtual source at the center of the intersection and capturing local street variables, such as main street width, side street width, as well as distance from gateway antenna to the main street wall, it has been reported that

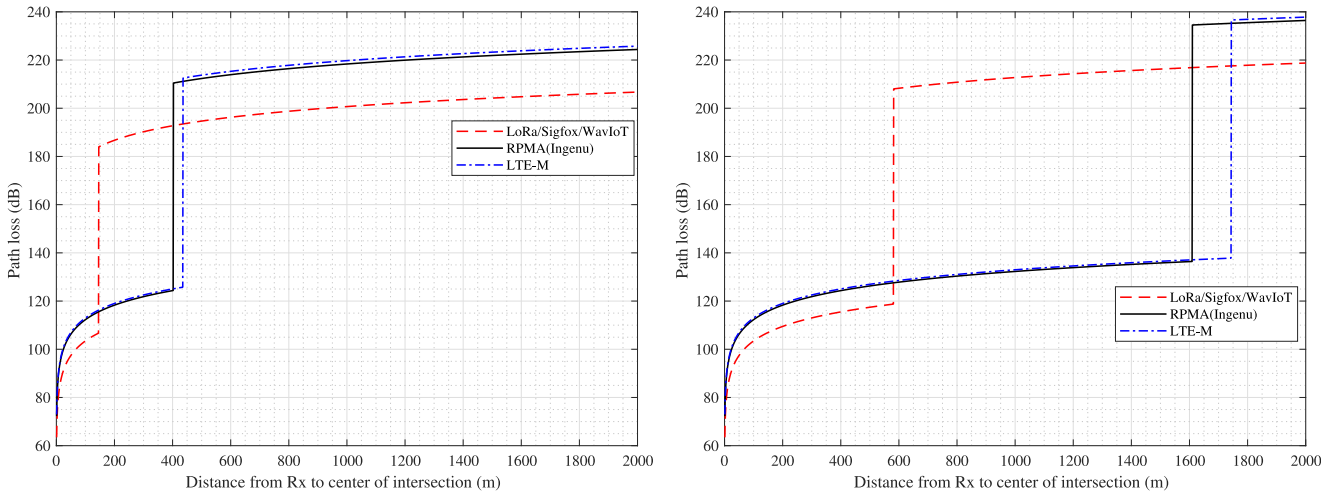


Fig. 5. NLOS path loss in urban environment with $S = f^{-0.024}$ [69], $\delta = 7$, $w_t = 7$, $x_t = 2$. (a) Gateway height 8 m, end device height 0.5 m. (b) Gateway height 8 m, end device height 2 m.

the NLOS path loss can be written as [71], [72]

$$\mathrm{PL}_{\mathrm{NLOS}} = \begin{cases} 10.\log_{10}\left(\frac{1}{\delta}\left(\sqrt{\frac{2\pi}{w_t.x_t}}.\frac{4\pi x_1 x_2}{\gamma}\right)\right)^2, & d \le d_c \\ 10.\log_{10}\left(\frac{1}{\delta}\left(\sqrt{\frac{2\pi}{w_t.x_t}}.\frac{4\pi x_1 x_2^2}{\gamma.d_c}\right)\right)^2, & d > d_c \end{cases} \tag{14}$$

where $w_t$, $x_t$ are the main street width and distance from gateway to the wall, respectively. While (13) includes the waveguide and 1-turn corner-turning effects of the path, (14) captures local street characteristics in addition. We have chosen $w_t$ to cater for shared surface street (used by pedestrians and vehicles in U.K., minimum 4.8 m [73]) and assume a regular shaped junction such that main and side streets are of equal widths.

Fig. 5 illustrates the effects of $d_c$ and street characteristics on NLOS path loss in urban street canyons for low and medium altitude IoT applications. The path loss significantly increases when $d > d_c$. In other words, reflection dominates the path loss when the receiving end device is close to the street junction, up to the cross over distance $d_c$. This is because the rays from the main street bend and arrive on the side street at an incidence angle close to 90° which results in very little or no refraction. Thereafter, the signals are reflected multiple times as they propagate further down the side street. Hence, for end devices located far from the junction, (beyond $d_c$), the path loss is dominated by diffraction. By increasing the height of the end device from 0.5 to 2 m, Fig. 5 shows that the path loss immediately after $d_c$ in LoRa (146 m), RPMA (403 m), and LTE-M (436 m) can be reduced by 77.24, 86.07, and 86.78 dB, respectively.

## VI. Network Performance Analysis

In this section, we compare performance of the various LPWAN technologies using the system parameters in each specification according to its data sheet and the scenario in the previous section. A sensitivity analysis is also conducted for each specification in urban area. The outcomes provide useful insights for attaining the tradeoff between network optimization and design complexity on one hand and cost on the other. We also examine the energy consumption and its dependencies in different use-cases. The battery life and energy consumption discussed in this section are with respect to the radio transceiver and includes transmit and receive consumption only. Other device components, such as micro-controller unit, wait windows, sleep currents, and other latent consumption in the system are not included.

### A. Coverage

One of the key performance metrics in wireless systems is the communication range. Given the scale of IoT in terms of applications, one of the challenges is how to ensure that the selected access technology is capable of providing adequate coverage for the area of interest. While coverage is relatively less constrained in rural and open areas, it is more challenging in large urban environments, such as metropolitan areas with heavy presence of high-rise modern buildings, road side furniture, such as street lights (lamp posts) and other man-made obstacles that reduce signal strength. By substituting (8)–(11) into (7), the maximum range can be expressed as

$$R = 10^{\frac{(P_t + \mathrm{Gain}_{\mathrm{net}} - \sigma - y_1 + y_2 + k_t)}{b_h}} \tag{15}$$

where $y_1 = 69.55 + 26.16 \cdot \log_{10} f$, $y_2 = 13.82 \cdot \log_{10} h_g$, $k_t = a(h_t) + c_t$ and $b_h = 44.9 - 6.55 \cdot \log_{10} h_g$.

Fig. 6 illustrates the maximum range achievable in rural and suburban areas using the main access technology specifications outlined in Table II. In particular, this figure shows that the coverage of each technology is dependent on the transmit power. In practice, coverage will vary among sites depending on the field characteristics. For example, the presence of multiple obstacles, such as trees or walls along the propagation path will also add to the attenuation of signal power. It is seen in Fig. 6 that in rural areas, using equal transmit power in the specifications considered, NB-IoT offers a significantly wider coverage (57.79 km at 40 dBm) than LTE-M (8.57 km at 40 dBm) in the cellular

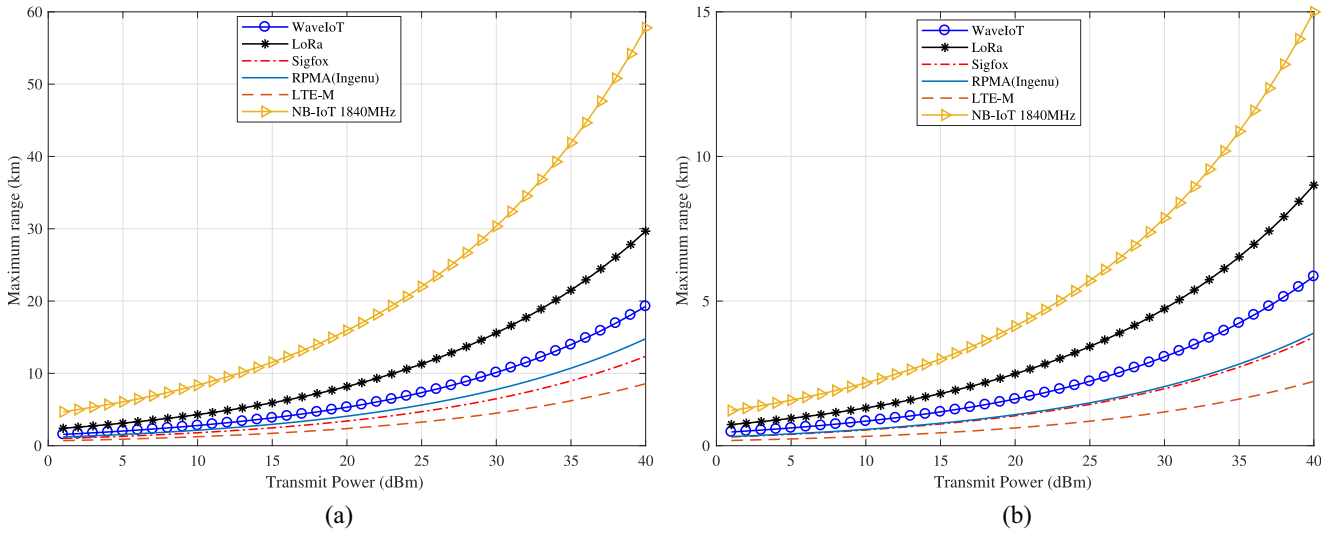


Fig. 6. Maximum range in (a) rural and (b) suburban areas.

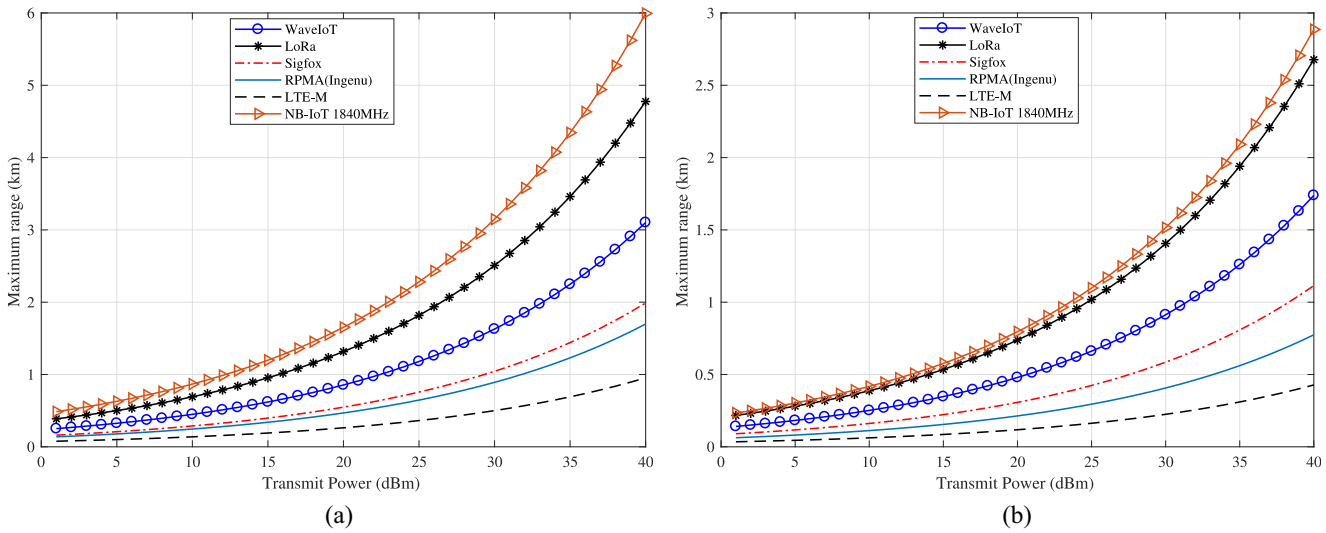


Fig. 7. Maximum range of access technologies in urban environments. (a) Range in small cities. (b) Range in large cities and metropolises.

domain while LoRaWAN offers the longest range (29.67 km) among the noncellular LP-WAN technologies. Overall, NB-IoT provides the widest coverage out of the six specifications considered. Although, Table II indicates that LTE-M and RPMA provide higher link budget than LoRaWAN, the low obstacle loss in LoRaWAN means that given the same transmit power and operating condition, it is more resilient to obstructions which improves the signal power reaching the end device from the gateway. On the other hand, even with lower transmit power of NB-IoT than LTE-M, the former relies on its better sensitivity and higher antenna gain to significantly extend the network coverage.

Similarly, the range in urban environment is illustrated in Fig. 7. The figure shows coverage of 2.89 km (NB-IoT), 2.68 km (LoRa), and 1.74 km(WavIoT) in large urban areas, meaning that NB-IoT end device can receive signal farther away from the gateway than LTE-M while LoRa receives the farthest signal among the noncellular technologies. Thus, the sub-GHz technologies are particularly beneficial in rural areas, where masts are less likely to be spread out. They also have some advantages in cities, because the sub-GHz technologies have lower penetration losses across brick walls, vegetation, concrete, metals, etc, which is suitable for underground applications, such as standpipe monitoring. As we move from small to large cities, the performance of RPMA further diverges from Sigfox. This is mainly due to their lower resilience to obstacle losses in large urban areas. Fig. 7 shows that RPMA and LTE-M are poor at traveling over long distances, which requires the towers to be closer together to deliver reliable coverage. Hence, 2.x GHz technologies may be less attractive in some rural deployments and deep indoor applications. Given the wide range of frequency and different modes of deployment supported by NB-IoT, it can be used in >GHz band or sub-GHz to cater for IoT connectivity in different terrains. In [32], the field experiments using LoRa deployment to cover the city of Padova in Italy reported a network coverage of about 1.2 km. This closely aligns with our result for small cities

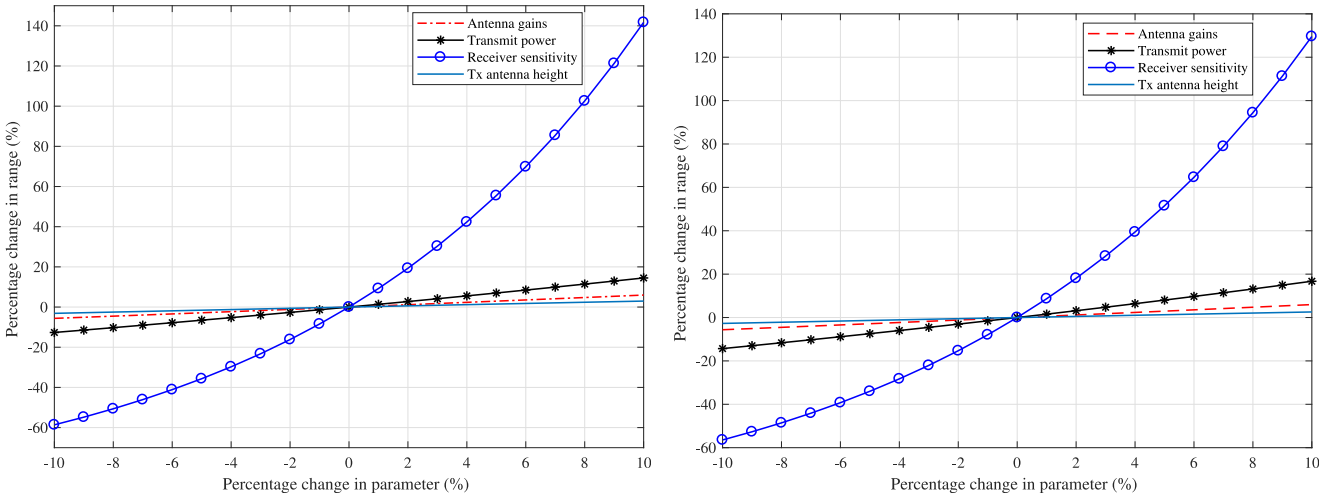


Fig. 8. Maximum range of (a) LoRaWAN and (b) Sigfox in urban environments.

TABLE V
RSSI AND SNR FOR SUBURBAN ENVIRONMENTS AT DIFFERENT DISTANCES FOR VARIOUS ACCESS TECHNOLOGIES

| Spec. | WAVIoT | LoRaWAN | Sigfox | RPMA | LTE-M |
|---|---|---|---|---|---|
| EIRP | 27 | 27 | 27 | 27 | 47 |
| $PL_{10}$ | 136.5 | 136.5 | 136.5 | 144.9 | 145.5 |
| $PL_{20}$ | 147.3 | 147.3 | 147.3 | 155.6 | 156.3 |
| $RSSI_{10}$ | -109.5 | -109.5 | -109.5 | -117.9 | -98.5 |
| $RSSI_{20}$ | -120.3 | -120.3 | -120.3 | -120.6 | -109.3 |
| $SNR_{10}$ | 20.5 | 20.5 | 20.5 | 12.1 | 31.5 |
| $SNR_{20}$ | 9.7 | 9.7 | 9.7 | 9.4 | 20.7 |

in Fig. 7(a) (1.4 km) based on LoRaWAN system specification with gateway transmit power of 21 dBm employed in this paper. Figs. 6 and 7 show that the 868 MHz technologies for instance do not exhibit the same coverage performance even when operated at the same frequency and equal transmit power. This is mainly due to the differences in the systems design and configurations.

For each technology type, the equivalent isotropically radiated power (EIRP) and SNR are also calculated. The EIRP is the output power radiated from the tip of the gateway antenna. Using the PL results in Fig. 3, the EIRP and nominal SNR for suburban environment at different link distances are summarized in Table V (for the downlink only).

In many wireless systems, such as Wi-Fi, the target SNR is usually 20 dB or higher to ensure reliable communication [63]. However, as seen in Table V, at link distance of 20 km, Sigfox and LoRaWAN yield SNR of 9.7 dB while RPMA offered 9.4 dB. These low SNR values are indications that the connectivity between IoT end point and gateway may be impaired with high frame error rate which will ultimately result in suboptimal link performance. In order to provide remedies for this condition, the following options can be explored.

1) Improve receiver sensitivity.
2) Increase the transmit power.
3) Use higher gain antenna.
4) Where possible, remove obstacles or other sources of losses.
5) Increase the antenna height.
6) Increase gateway density by deploying more base stations which will reduce the distance from gateway to IoT end point.

Some of these factors are investigated as part of the sensitivity analysis in the next section.

### B. Sensitivity Analysis and Network Optimization

We observed from Fig. 7 that coverage limitation is more imminent in urban areas, therefore the objective of this section is to investigate ways to optimize network performance by conducting a sensitivity analysis. Equations (11) and (15) as well as their dependence on field parameters suggest that some variables can be tuned to optimize performance of the communication network. As the current LP-WAN specifications employ different values of system parameters, percentage changes are employed instead of absolute values. In each case, a variable is changed by a fixed percentage and the resultant improvement or degradation in the network coverage is estimated. Thus, the transmit power, antenna gain, receiver sensitivity, and the height of gateway antenna are varied within $\pm 10\%$ in succession.

Figs. 8 and 9, respectively, illustrates the coverage gain in large cities and metropolitan areas. In each case, the outcome is compared among four access technologies and it can be seen that the network responds to the changes in different degrees. In Fig. 8, LoRaWAN and Sigfox exhibit similar performance and trend until 3% change in system parameter. Beyond that point, LoRaWAN outperforms Sigfox and this is more pronounced from 8%–10%, where LoRaWAN provides more coverage gain. LP-WAN transceivers are engineered to be very sensitive. As a result, the end points can detect signals that are smaller than transmit power by many order of magnitude. Fig. 8, however, shows that by increasing the receiver sensitivity by 10%, LoRaWAN and Sigfox can extend coverage by 141.7% and 129.57%, respectively, meaning a comparative gain of 12.13% in favor of LoRaWAN. Furthermore, Fig. 9 illustrates the additional coverage gain when similar parameters are varied in RPMA and LTE-M. It is observed that a 10% improvement in receiver

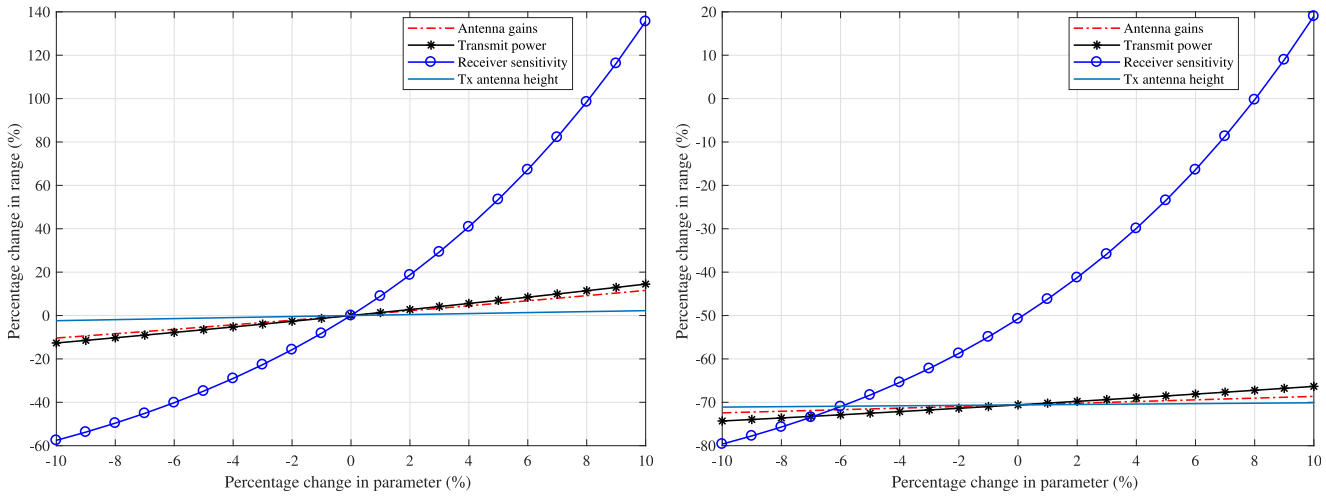


Fig. 9. Coverage optimization with 2.4 GHz and 2.6 GHz LTE in urban environments. (a) RPMA (2.4 GHz ISM). (b) LTE-M (2.6 GHz).

sensitivity can increase coverage by 135.56% in RPMA and 19% in LTE-M. It is further noted that increase in transmit power alone yields about 17% coverage improvement in the best case [Fig. 9(a)].

Similarly in Fig. 10, it is observed that with a 10% improvement in NB-IoT 882 MHz receiver sensitivity, coverage can increase by about 398% while a similar change in transmit power and antenna gain yields 130% and 122%, respectively. In the case of NB-IoT 1840 MHz, a 10% improvement in sensitivity yields about 191% coverage gain while a similar change in transmit power and antenna gain enhance coverage by about 34% and 30%, respectively. Based on the specifications and parameters employed in this paper, we can see in Figs. 8–10 that among the system parameters employed, receiver sensitivity and transmit power are two of the key parameters for optimizing LP-WAN coverage. This approach affords the opportunity to identify the most sensitive parameters. With such knowledge, system designers and engineers can explore further ways of tweaking the identified parameters in a manner that is cost-effective without compromising network reliability, power requirement or other key performance indicators of the access networks.

While increase in antenna gain, transmit power and antenna height can improve the received signal level, they also increase the chances of higher interference. Therefore, the pros and cons of each optimization approach needs to be carefully considered.

### C. Transmission Delay

The transmission delay of a message of length $|\Psi|$ bits can be determined from Shanon–Hartley theorem as

$$\tau(\varepsilon, \sigma, |\Psi|) = \frac{|\Psi|}{\varepsilon} \cdot \log_2\left(1 + \varepsilon^{-1}.\frac{\beta\sigma}{\phi N_0}\right) \tag{16}$$

where $\sigma(\text{dBm}) = P_t - \alpha$ is the receiver sensitivity ($P_t$ is the transmit power and $\alpha$ is the coupling loss), $\beta$ is a correction factor to account for difference between Shanon limit and realistic systems and $N_0$ is the thermal noise power spectral density which is about $-174$ dBm/Hz. The minimum time required to transmit message $A$ is achieved when $\varepsilon \longrightarrow \infty$. This is supported by the fact that larger bandwidth causes messages to be transmitted faster such that [74]

$$\tau(\infty, \sigma, |\Psi|) = \ln 2.|\Psi|\left(\frac{\beta\sigma}{\phi N_0}\right)^{-1}. \tag{17}$$

Equations (16) and (17) further imply that given a fixed receiver sensitivity in each LP-WAN specification, the transmission delay depends on the data rate and message length. Sending 50 byte payload in LoRaWAN in Europe in some cases can take approximately 2.8 s using the minimum data rate (SF12) and 0.154 s using the maximum data rate (SF7). This means that the end devices have to wait 4 min 37 s after each transmission in the former and 15.25 s in the latter. However, Fig. 11 indicates that if the payload size is reduced by 20%, the time-on-air (ToA) can decrease by 328 and 61.44 ms for SF12 and SF7, respectively.

ToA for LoRaWAN is significantly affected by both payload size and SF. However, as seen in Fig. 11, the impact of SF is higher than that of the payload, which implies that for a given payload, the ToA increases more rapidly with the SF value. The reason is that SF 7 and SF 12 offer the highest and lowest data rates, respectively. Therefore, increasing the SF is equivalent to reducing the network throughput and if all other parameters remain unchanged, the penalty for that is higher ToA which will also impact the end-to-end latency experienced by the software (application).

### D. Energy Consumption

To investigate the energy consumption of the IoT end devices, this paper adopts the first order radio energy dissipation model introduced in [55] and subsequently applied in other studies, such as [56] and [75]. In estimating the battery life of the transceivers, we adopt the E91-AA alkaline battery model and apply its operational characteristics [76]. According to [55], the transmitter consumes energy to operate the radio electronics and the power amplifier while the receiver consumes energy to run the radio electronics as shown in Fig. 12.

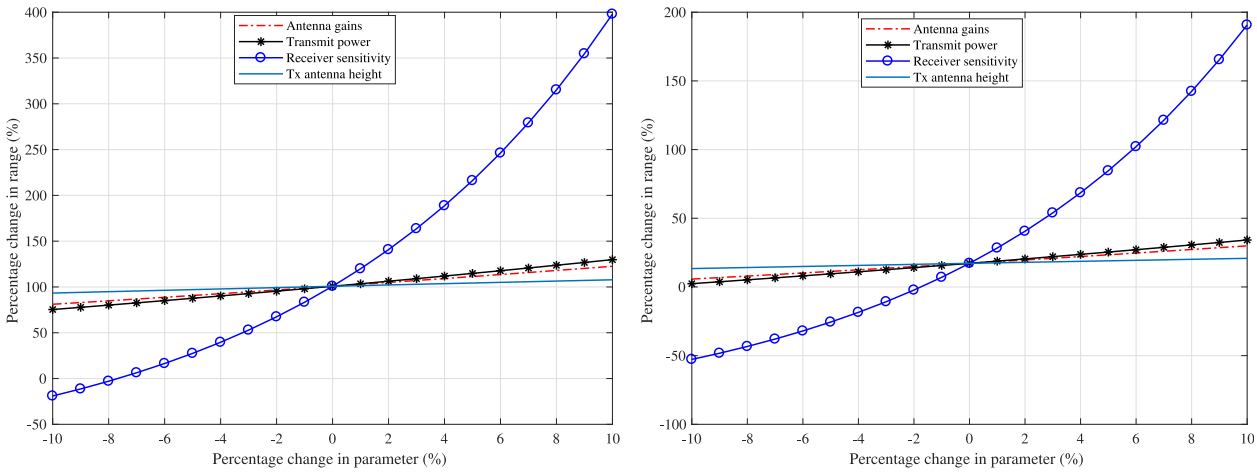


Fig. 10. Range optimization with NB-IoT at (a) 882 MHz and (b) 1840 MHz, bands 5 and 3 downlink frequency, respectively, 3GPP NB-IoT (rel. 13) [49].

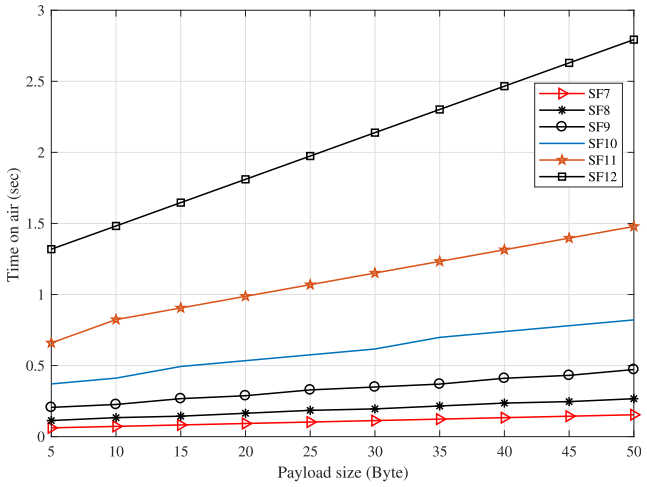


Fig. 11. Time on air of LoRaWAN messages versus payload size with coding rate 4/5, preamble symbols 8, bandwidth 125 kHz, duty cycle 0.1%.

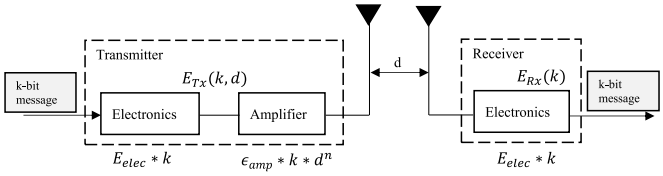


Fig. 12. First order radio energy dissipation model.

The energy required to transmit a $k$-bit message from the IoT end device to the gateway over a distance $d$ can be defined as

$$E^{\mathrm{Tx}}(k,d) = E^{\mathrm{Tx}}_{\mathrm{elec}}(k) + E^{\mathrm{Tx}}_{\mathrm{amp}}(k,d) \tag{18}$$

where $E^{\mathrm{Tx}}_{\mathrm{elec}}$ is the electrical energy consumed by the electronic circuit of the transmitter radio and depends on signal processing techniques, such as modulation, spreading, and coding, while $E^{\mathrm{Tx}}_{\mathrm{amp}}$ is the communication-related energy consumed by the amplifier which depends on the environmental factors including the distance from transmitter to receiver. At the receiver, since

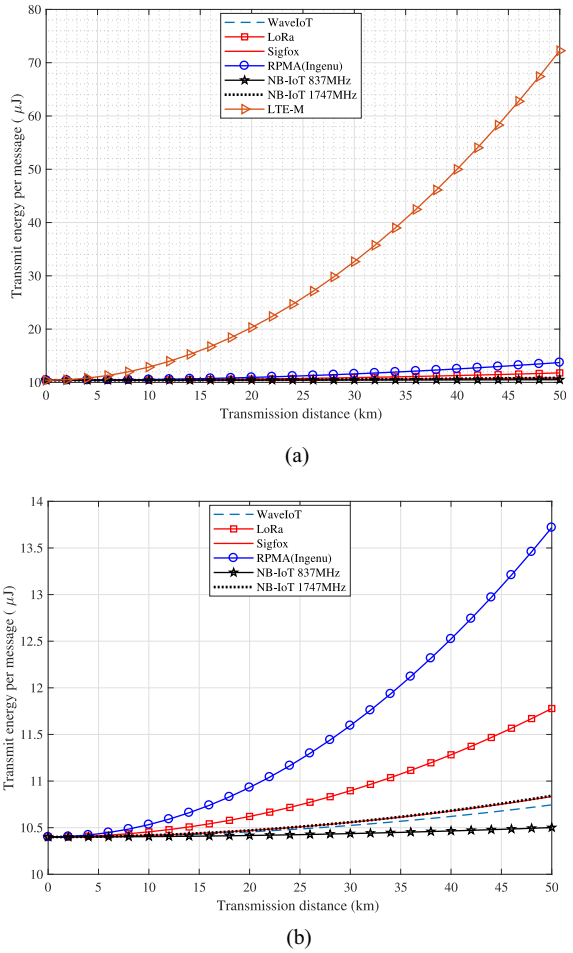


Fig. 13. Transmit energy consumed per message using gateway height of 12 m and end device height of 0.5 m, data rate 100 b/s, and payload of 12 bytes. (a) Comparing transmit energy for WavIoT, LoRa, Sigfox, RPMA, LTE-M, and NB-IoT. (b) Enlarged Fig. 11(a) showing WavIoT, LoRa, Sigfox, RPMA, and NB-IoT.

the radio only needs energy to operate the electronics to detect the signal, the energy consumed is

$$E^{\mathrm{Rx}}(k) = E^{\mathrm{Rx}}_{\mathrm{elec}}(k) = k \cdot E_{\mathrm{elec}}. \tag{19}$$

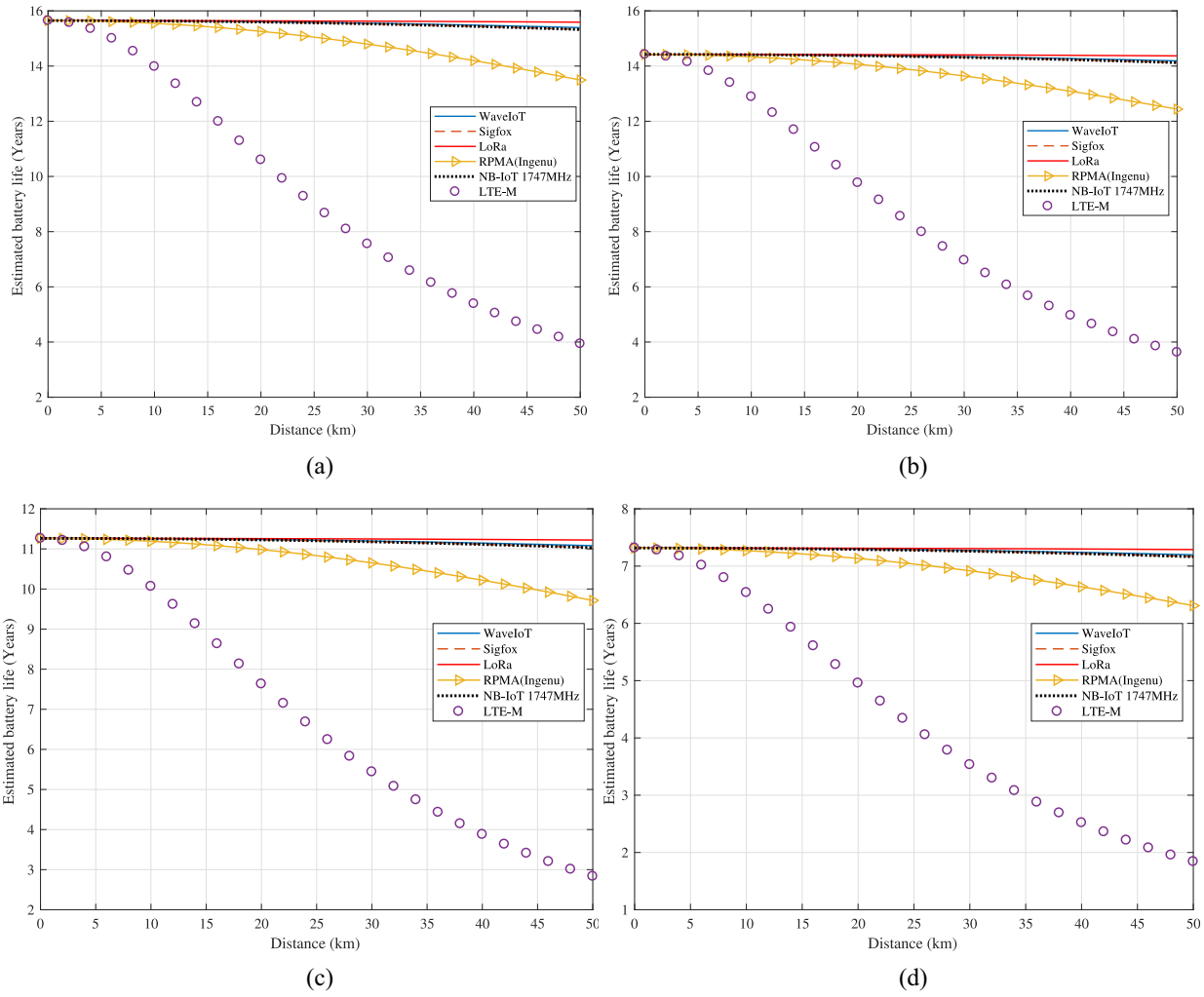


Fig. 14. Estimated battery life in LP-WAN transceiver operating at 1% duty cycle under different weather conditions, using gateway height of 12 m and end device height of 0.5 m, data rate 100 b/s, and payload of 12 bytes. Device battery operating at (a) 40 °C, (b) 20 °C, (c) 0 °C, and (d) −20 °C.

Both the free space and multipath-fading channels are considered in the energy model, depending on the distance between the gateway and end device. If the transmission distance is less than a certain threshold $d_c$, the free space model ($d^2$ power loss) is used, otherwise the multipath model ($d^4$ power loss) applies [55]. Therefore, power control can be employed to invert this loss by setting the power amplifier value of $E_{\text{amp}}^{\text{Tx}}$ at the transmitter in a way that ensures that adequate signal power arrive at the receiver. Thus, the transmitter energy consumption can be written as

$$E^{\text{Tx}}(k,d) = \begin{cases} k\left(E_{\text{elec}}^{\text{Tx}} + \epsilon_{\text{Friis}} d^2\right), & d < d_c \\ k\left(E_{\text{elec}}^{\text{Tx}} + \epsilon_{\text{Two-ray}} d^4\right), & d \geq d_c \end{cases} \tag{20}$$

where the threshold distance is define as $d_c = 4\pi\sqrt{L}(h_g h_t/\gamma)$, $L \geq 1$ is the system loss factor and $\gamma$ is the wavelength of the signal. Applying the parameters in Table II, if the gateway is 12 m high and the end device is 0.5 m (low altitude applications, such as smart agriculture and smart cities) with $L = 1$ (assume no system loss), the $d_c$ for WavIoT/Sigfox/LoRa, RPMA and LTE-M are 218.18 m, 603.26 m and 653.54 m, respectively.

Fig. 13 compares the transmit energy consumed per message for the LP-WAN technologies considered in this paper. It can be seen that overall, LTE-M consumes the highest amount of energy for every message sent by the IoT end device, followed by RPMA. For distances below 2 km, the technologies consume approximately equal amount of energy. However, beyond 2 km, the performance gap increases rapidly with distance.

Here, we apply a duty cycle of 1% (corresponding to 140 messages per day) to the devices to conform with the regulatory requirements in Europe and analyze the energy consumption of the devices. Fig. 14 presents the estimated battery life in the devices when deployed with the LP-WAN technologies and operated at different temperatures. This figure shows clearly that the operating temperature is a key determinant of battery life. In particular, extremely cold temperature can significantly shorten the active lifespan of the end device due to rapid degradation of its battery's capacity. Nevertheless, based on the configurations employed in this section, LoRa appears to be the most promising to support long battery life while LTE-M provides the shortest battery life across the temperatures investigated. For example, with a coverage requirement of 25 km, Fig. 14 shows that at 40 °C, LoRaWAN, Sigfox, NB-IoT, and WavIoT can each support up to 15.65 years while RPMA and LTE-M devices are active for 14.9 and 8.8 years,

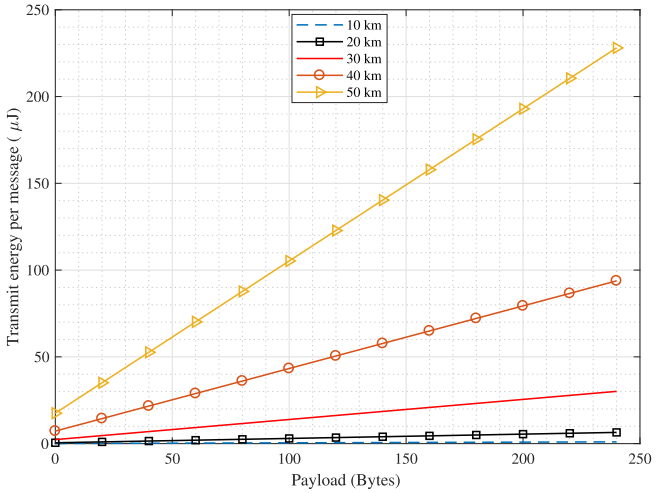


Fig. 15. Effects of payload size on daily energy consumption for different coverage requirements in LoRaWAN using gateway height 12 m, end device height 0.5 m, duty cycle of 1%, and data rate of 25 kb/s.

respectively. However, when the temperature drops to −20 °C, the figure indicates that the battery life reduces to about 7.32 years for LoRaWAN, Sigfox, and WavIoT as well as 7 and 4.2 years for RPMA and LTE-M, respectively. These results generally suggest that even with the same system configurations and battery capacity when IoT devices are deployed, their active lifetimes will vary across regions according to the local temperature and seasonal variations. These results can potentially offer useful insights into the planning, designing, and management of the IoT access networks, especially in use-cases, such as haulage/logistics, smart agriculture, and many smart city scenarios in which the sensors may be unavoidably exposed to extreme weather conditions.

In Fig. 15, we present the variation of daily transmit energy consumption with payload size for different coverage requirements using LoRaWAN. Although the effect of distance is generally more pronounced, the figure indicates that energy required is significantly affected by message size as well. For example, for a coverage distance of 50 km, reducing the message size by 20% can result in transmit energy savings of about 47 $\mu$J per message and this can extend the device life. The availability of SF in LoRaWAN provides a way to further trade-off between system variables and energy consumption, thereby offering additional degree of flexibility in IoT access network design.

## VII. Conclusion

Current IoT access technologies are optimized for different end-use applications. This paper showed that each of RPMA and LTE-M incur at least 9 dB additional path loss compared with Sigfox and LoRAWAN. That means they are more suitable for short range applications. In real deployments, the alternatives include the use of higher gain antennas or reduction of coverage per gateway both of which impact the deployment cost.

To illustrate the consequences of link budget on system performance, parameters were adopted from the LP-WAN datasheets. The results consistently indicated that receiver sensitivity is the most significant variable in LP-WAN optimization, followed by transmit power. For example, it was shown that with a 10% improvement in receiver sensitivity, LoRaWAN can increase network coverage by about 142% and Sigfox by 130%, whereas with similar receiver sensitivity in NB-IoT 882 MHz and LTE-M, the coverage gains were about 398% and 136%, respectively.

Across the technologies, the active device life is affected by payload size, distance, and environmental conditions, such as temperature. In addition to the applied load, it was observed that extreme weather conditions can significantly reduce active device life of IoT objects in the LP-WAN. Compared with environmental temperature of 40 °C, the results indicate operating the IoT devices at a temperature of −20 °C, can reduce the device life by about half; 53% (WavIoT, LoRaWAN, Sigfox, RPMA) and 48% in LTE-M. Indoor signal propagation is remarkably different from outdoor due to the plethora of objects contributing to the interference level as well as attenuation from different objects some of which are outlined in Table IV. Thus, our future work in this area includes the investigation of the effects of indoor losses on IoT network performance using the LP-WAN technologies discussed in this paper and any future ones available.

## Nomenclature

| | |
|---|---|
| $\alpha$ | Coupling loss. |
| $\beta$ | Correction factorbetween Shanon limit and realistic systems. |
| $\delta$ | Environmental parameter. |
| $\epsilon_{\text{Friis}}$ | Dissipation variable, free space. |
| $\epsilon_{\text{Two-ray}}$ | Dissipation variable, multi-path fading. |
| $\eta$ | Receiver sensitivity. |
| $\gamma$ | Wavelength. |
| $\lambda$ | Gateway density. |
| $\phi$ | Noise figure. |
| $\sigma$ | Receiver sensitivity. |
| $\theta$ | Threshold SNR. |
| $\varepsilon$ | Bandwidth. |
| $\varphi$ | Viewing angle from gateway to end device antenna |
| $\Psi$ | Message length. |
| $a(h_t)$ | Terrain parameter. |
| $C$ | Channel capacity. |
| $c_t$ | Terrain correction factor. |
| $d_c$ | Cross-over distance. |
| $E_{\text{amp}}^{\text{Tx}}$ | Electrical energy consumed by transmitting radio amplifier. |
| $E_b$ | Energy per bit. |
| $E_{\text{elec}}$ | Electrical energy consumed by radio electronic circuit. |
| $G_{\text{net}}$ | Net gain. |
| $h_g$ | Gateway antenna height. |
| $N_0$ | Thermal noise power. |
| $P_t$ | Transmit power. |
| $w_t$ | Width of main street. |
| $x_t$ | Distance: gateway antenna to wall on main street. |

## REFERENCES


[1] Statistica. (2015). *Internet of Things (IoT) Connected Devices Installed Base Worldwide From 2015 to 2025 (in Billions)*. Accessed: May 26, 2018. [Online]. Available: https://www.statista.com/statistics/471264/iot-number-of-connected-devices-worldwide/

[2] M. James *et al.* (2015). *Unlocking the Potential of the Internet of Things*. Accessed: May 26, 2018. [Online]. Available: https://www.mckinsey.com/business-functions/digital-mckinsey/our-insights/the-internet-of-things-the-value-of-digitizing-the-physical-world

[3] Drives and Controls. (2017). *1 in 4 Wireless IIoT Connections Will Use LPWA By 2025*. Accessed: May 26, 2018. [Online]. Available: http://m.drivesncontrols.com/news/fullstory.php/aid/5553/1_in_4_wireless_IIoT_connections_will_use_LPWA_by_2025.html

[4] T. M. Wg. (2015). *A Technical Overview of LoRa and LoRaWAN*. Accessed: Jan. 29, 2018. [Online]. Available: https://docs.wixstatic.com/ugd/eccc1a_ed71ea1cd969417493c74e4a13c55685.pdf

[5] K. E. Nolan, W. Guibene, and M. Y. Kelly, "An evaluation of low power wide area network technologies for the Internet of Things," in *Proc. IEEE Int. Wireless Commun. Mobile Comput.*, 2016, pp. 439–444.

[6] U. Raza, P. Kulkarni, and M. Sooriyabandara, "Low power wide area networks: An overview," *IEEE Commun. Surveys Tuts.*, vol. 19, no. 2, pp. 855–873, 2nd Quart., 2017.

[7] N. Poursafar, M. E. E. Alahi, and S. Mukhopadhyay, "Long-range wireless technologies for IoT applications: A review," in *Proc. IEEE Int. Conf. Sens. Technol.*, Dec. 2017, pp. 1–6.

[8] J. de Carvalho Silva, J. J. P. C. Rodrigues, A. M. Alberti, P. Solic, and A. L. L. Aquino, "LoRaWAN—A low power WAN protocol for Internet of Things: A review and opportunities," in *Proc. IEEE Int. Multidiscipl. Conf. Comput. Energy Sci. (SpliTech)*, Jul. 2017, pp. 1–6.

[9] K. Mekki, E. Bajic, F. Chaxel, and F. Meyer, "A comparative study of LPWAN technologies for large-scale IoT deployment," *ICT Exp.*, vol. 12, no. 5, 2018. [Online]. Available: https://www.sciencedirect.com/science/article/pii/S2405959517302953

[10] M. Aazam, S. Zeadally, and K. A. Harras, "Offloading in fog computing for IoT: Review, enabling technologies, and research opportunities," *Future Gener. Comput. Syst.*, vol. 4, no. 57, pp. 278–289, 2018.

[11] S. Al-Sarawi, M. Anbar, K. Alieyan, and M. Alzubaidi, "Internet of Things (IoT) communication protocols: Review," in *Proc. IEEE Int. Conf. Inf. Technol.*, May 2017, pp. 685–690.

[12] K. Zheng, S. Zhao, Z. Yang, X. Xiong, and W. Xiang, "Design and implementation of LPWA-based air quality monitoring system," *IEEE Access*, vol. 4, pp. 3238–3245, 2016.

[13] W. Guibene *et al.*, "Evaluation of LPWAN technologies for smart cities: River monitoring use-case," in *Proc. IEEE Wireless Commun. Netw. Conf. Workshops (WCNCW)*, 2017, pp. 1–5.

[14] J. Chen *et al.*, "Narrowband Internet of Things: Implementations and applications," *IEEE Internet Things J.*, vol. 4, no. 6, pp. 2309–2314, Dec. 2017.

[15] W. Guibene, K. E. Nolan, and M. Y. Kelly, "Survey on clean slate cellular-IoT standard proposals," in *Proc. IEEE Int. Conf. Comput. Inform. Technol. Ubiquitous Comput. Commun. Depend. Auton. Secure Comput. Pervasive Intell. Comput. (CIT/IUCC/DASC/PICOM)*, 2015, pp. 1596–1599.

[16] F. Adelantado *et al.*, "Understanding the limits of LoRaWAN," *IEEE Commun. Mag.*, vol. 55, no. 9, pp. 34–40, Sep. 2017.

[17] L. Gregora, L. Vojtech, and M. Neruda, "Indoor signal propagation of LoRa technology," in *Proc. Int. Conf. Mechatronics Mechatronika (ME)*, 2016, pp. 1–4.

[18] B. Reynders, W. Meert, and S. Pollin, "Power and spreading factor control in low power wide area networks," in *Proc. Int. Conf. Commun. (ICC)*, 2017, pp. 1–6.

[19] N. Mangalvedhe, R. Ratasuk, and A. Ghosh, "NB-IoT deployment study for low power wide area cellular IoT," in *Proc. IEEE Annu. Int. Symp. Pers. Indoor Mobile Radio Commun.*, 2016, pp. 1–6.

[20] J. Petajajarvi, K. Mikhaylov, A. Roivainen, T. Hanninen, and M. Pettissalo, "On the coverage of LPWANs: Range evaluation and channel attenuation model for LoRa technology," in *Proc. IEEE Int. Conf. ITS Telecommun.*, 2015, pp. 55–59.

[21] M. Aref and A. Sikora, "Free space range measurements with Semtech LoRa$^{TM}$ technology," in *Proc. 2nd Int. Symp. Wireless Syst. Conf. Intell. Data Acquisition Adv. Comput. Syst.*, 2014, pp. 19–23.

[22] M. Lauridsen, I. Z. Kovács, P. Mogensen, M. Sorensen, and S. Holst, "Coverage and capacity analysis of LTE-M and NB-IoT in a rural area," in *Proc. IEEE Veh. Tech Conf.*, 2016, pp. 1–5.

[23] O. Georgiou and U. Raza, "Low power wide area network analysis: Can LoRa scale?" *IEEE Wireless Commun. Lett.*, vol. 6, no. 2, pp. 162–165, Apr. 2017.

[24] Y. Mo, C. Goursaud, and J.-M. Gorce, "Theoretical analysis of UNB-based IoT networks with path loss and random spectrum access," in *Proc. IEEE Int. Symp. Pers. Indoor Mobile Radio Commun.*, 2016, pp. 1–6.

[25] H. Mroue *et al.*, "MAC layer-based evaluation of IoT technologies: LoRa, SigFox and NB-IoT," in *Proc. IEEE Middle East North Africa Commun. Conf. (MENACOMM)*, 2018, pp. 1–5.

[26] M. D'Aloia *et al.*, "An innovative LPWA network scheme to increase system reliability in remote monitoring," in *Proc. IEEE Environ. Energy Struct. Monitor. Syst. (EESMS) Workshop*, 2017, pp. 1–6.

[27] S. Gangakhedkar, O. Bulakci, and J. Eichinger, "Addressing deep indoor coverage in narrowband-5G," in *Proc. IEEE Veh. Technol. Conf.*, 2017, pp. 1–5.

[28] C. Y. Yeoh, A. bin Man, Q. M. Ashraf, and A. K. Samingan, "Experimental assessment of battery lifetime for commercial off-the-shelf NB-IoT module," in *Proc. IEEE Int. Conf. Adv. Commun. Techn.*, 2018, p. 1.

[29] A. Augustin, J. Yi, T. Clausen, and W. M. Townsley, "A study of LoRa: Long range & low power networks for the Internet of Things," *Sensors*, vol. 16, no. 9, p. 1466, 2016.

[30] K. Mikhaylov, J. Petaejaejaervi, and T. Haenninen, "Analysis of capacity and scalability of the LoRa low power wide area network technology," in *Proc. VDE Eur. Wireless Conf.*, 2016, pp. 1–6.

[31] M. Lauridsen *et al.*, "Coverage comparison of GPRS, NB-IoT, LoRa, and SigFox in a 7800 km$^2$ area," in *Proc. IEEE Veh. Technol. Conf.*, 2017, pp. 1–5.

[32] M. Centenaro, L. Vangelista, A. Zanella, and M. Zorzi, "Long-range communications in unlicensed bands: The rising stars in the IoT and smart city scenarios," *IEEE Wireless Commun.*, vol. 23, no. 5, pp. 60–67, Oct. 2016.

[33] H. Wang and A. O. Fapojuwo, "A survey of enabling technologies of low power and long range machine-to-machine communications," *IEEE Commun. Surveys Tuts.*, vol. 19, no. 4, pp. 2621–2639, 1st Quart., 2017.

[34] G. A. Akpakwu, B. J. Silva, G. P. Hancke, and A. M. Abu-Mahfouz, "A survey on 5G networks for the Internet of Things: Communication technologies and challenges," *IEEE Access*, vol. 6, pp. 3619–3647, 2018.

[35] M. Chen, Y. Miao, Y. Hao, and K. Hwang, "Narrow band Internet of Things," *IEEE Access*, vol. 5, pp. 20557–20577, 2017.

[36] P. Neumann, J. Montavont, and T. Noël, "Indoor deployment of low-power wide area networks (LPWAN): A LoRaWAN case study," in *Proc. IEEE Conf. Wireless Mobile Comput. Netw. Commun. (WiMob)*, 2016, pp. 1–8.

[37] K. Mikhaylov, J. Petäjäjärvi, and J. Janhunen, "On LoRaWAN scalability: Empirical evaluation of susceptibility to inter-network interference," in *Proc. IEEE Eur. Conf. Netw. Commun. (EuCNC)*, 2017, pp. 1–6.

[38] Mathuranathan. (2008). *Channel Capacity & Shannon Theorem—Demystified*. Accessed: Aug. 7, 2018. [Online]. Available: https://www.gaussianwaves.com/2008/04/channel-capacity/

[39] T. Myers. (2016). *Back to Basics: The Shannon–Hartley Theorem*. Accessed: Dec. 17, 2017. [Online]. Available: https://www.ingenu.com/2016/07/back-to-basics-the-Shannon-Hartley-theorem/

[40] *LoRa Modulation Basics*, Semtech, Camarillo, CA, USA, 2015.

[41] A. AlAmmouri, J. G. Andrews, and F. Baccelli, "SINR and throughput of dense cellular networks with stretched exponential path loss," *IEEE Trans. Wireless Commun.*, vol. 17, no. 2, pp. 1147–1160, Feb. 2018.

[42] X. Zhang and J. G. Andrews, "Downlink cellular network analysis with multi-slope path loss models," *IEEE Trans. Commun.*, vol. 63, no. 5, pp. 1881–1894, May 2015.

[43] M. Di Renzo, W. Lu, and P. Guan, "The intensity matching approach: A tractable stochastic geometry approximation to system-level analysis of cellular networks," *IEEE Trans. Wireless Commun.*, vol. 15, no. 9, pp. 5963–5983, Sep. 2016.

[44] A. Al Ammouri, J. G. Andrews, and F. Baccelli, "A unified asymptotic analysis of area spectral efficiency in ultradense cellular networks," *IEEE Trans. Inf. Theory*, to be published, doi: 10.1109/TIT.2018.2845380.

[45] K.-H. Phung, H. Tran, Q. Nguyen, T. T. Huong, and T.-L. Nguyen, "Analysis and assessment of LoRaWAN," in *Proc. IEEE Int. Conf. Recent Adv. Sig. Process. Telecommun. Comput.*, 2018, pp. 241–246.

[46] Link-Labs. (2016). *A Comprehensive Look at Low Power, Wide Area Networks for Internet of Things Engineers and Decision Makers*. Accessed: Dec. 14, 2017. [Online]. Available: https://www.link-labs.com/symphony

[47] Ingenu. (2015). *An Educational Guide a White Paper by Ingenu How RPMA Works*. Accessed: Dec. 14, 2017. [Online]. Available: http://www.ingenu.com
[48] WavIOT. (2017). *Comparison of LPWAN Technologies*. Accessed: Dec. 23, 2017. [Online]. Available: https://waviot.com/wp.pdf
[49] J. Schlienz and D. Raddino, *Narrowband Internet of Things Whitepaper*, Rohde & Schwarz, Munich, Germany, 2016. Accessed: Aug. 3, 2018. [Online]. Available: https://cdn.rohde-schwarz.com/pws/dl_downloads/dl_application/application_notes/1ma266/1MA266_0e_NB_IoT.pdf
[50] A. Ratilainen. (2016). *NB-IoT Presentation for IETF LPWAN*. Accessed: Aug. 3, 2018. [Online]. Available: https://datatracker.ietf.org/meeting/97/materials/slides-97-lpwan-30-nb-iot-presentation-00
[51] R. Ratasuk, J. Tan, N. Mangalvedhe, M. H. Ng, and A. Ghosh, "Analysis of NB-IoT deployment in LTE guard-band," in *Proc. IEEE Veh. Technol. Conf. (VTC Spring)*, 2017, pp. 1–5.
[52] S.-M. Oh and J. Shin, "An efficient small data transmission scheme in the 3GPP NB-IoT system," *IEEE Commun. Lett.*, vol. 21, no. 3, pp. 660–663, Mar. 2017.
[53] D. M. Hernandez *et al.*, "Energy and coverage study of LPWAN schemes for industry 4.0," in *Proc. IEEE Int. Workshop Electron. Control Meas. Signals Appl. Mechatronics (ECMSM)*, 2017, pp. 1–6.
[54] G. G. L. Ribeiro *et al.*, "An outdoor localization system based on SigFox," in *Proc. IEEE Conf. Veh. Technol.*, 2018, pp. 1–5.
[55] W. B. Heinzelman, A. P. Chandrakasan, and H. Balakrishnan, "An application-specific protocol architecture for wireless microsensor networks," *IEEE Trans. wireless Commun.*, vol. 1, no. 4, pp. 660–670, Oct. 2002.
[56] Y. Zhuang, J. Pan, and G. Wu, "Energy-optimal grid-based clustering in wireless microsensor networks," in *Proc. IEEE Int. Conf. Distrib. Comput. Syst. Workshops*, 2009, pp. 96–102.
[57] SigFox. (2017). *SigFox Technical Overview*. Accessed: Mar. 7, 2018. [Online]. Available: https://www.element14.com/community/docs/DOC-87914/l/sigfox-technical-overview
[58] B. Vejlgaard *et al.*, "Interference impact on coverage and capacity for low power wide area IoT networks," in *Proc. IEEE Wireless Commun. Netw. Conf. (WCNC)*, 2017, pp. 1–6.
[59] Randallthorp. (2014). *West Carbourne Building Heights*. Accessed: Jun. 10, 2018. [Online]. Available: https://www.scambs.gov.uk/sites/default/files/documents/85S-77J%20BuildingHeights.pdf
[60] A. D. Zayas and P. Merino, "The 3GPP NB-IoT system architecture for the Internet of Things," in *Proc. IEEE Int. Conf. Commun. Workshops (ICC Workshops)*, 2017, pp. 277–282.
[61] A. Ikpehai, B. Adebisi, and A. Kelvin, "Effects of traffic characteristics on energy consumption of IoT end devices in smart city," in *Proc. IEEE Glob. Inf. Infrastruct. Netw. Symp.*
[62] H. Mazar, "L-O-S radio links, clearance above tall buildings," in *Proc. Conven. Elect. Electron. Eng. Israel*, 1991, pp. 145–148.
[63] Cisco. (2014). *Radio Frequency Fundamentals*. Accessed: Jan. 2, 2018. [Online]. Available: https://www.cisco.com/c/en/us/td/docs/solutions/Enterprise
[64] T. S. Rappaport *et al.*, *Wireless Communications: Principles and Practice*, vol. 2. Upper Saddle River, NJ, USA: Prentice-Hall, 1996.
[65] V. S. Abhayawardhana, I. J. Wassell, D. Crosby, M. P. Sellars, and M. G. Brown, "Comparison of empirical propagation path loss models for fixed wireless access systems," in *Proc. IEEE Veh. Tech. Conf*, vol. 1, 2005, pp. 73–77.
[66] W. Debus. (2006). *RF Path Loss & Transmission Distance Calculations*. Accessed: Jan. 16, 2018. [Online]. Available: https://pdfs.semanticscholar.org/f126/eb84e340cf74d63ab26782c9ad30cd111114.pdf
[67] M. Hata, "Empirical formula for propagation loss in land mobile radio services," *IEEE Trans. Veh. Technol.*, vol. VT-29, no. 3, pp. 317–325, Aug. 1980.
[68] Y. Okumura, E. Ohmori, T. Kawano, and K. Fukuda, "Field strength and its variability in VHF and UHF land-mobile radio-services," *Rev. Elect. Commun. Lab.*, vol. 16, pp. 825–873, Oct. 1968.
[69] J. S. Lu, H. L. Bertoni, K. A. Remley, W. F. Young, and J. Ladbury, "Site-specific models of the received power for radio communication in urban street canyons," *IEEE Trans. Antennas Propag.*, vol. 62, no. 4, pp. 2192–2200, Apr. 2014.
[70] J. Lee, M.-D. Kim, H. K. Chung, and J. Kim, "NLOS path loss model for low-height antenna links in high-rise urban street grid environments," *Int. J. Antennas Propag.*, vol. 2015, Jan. 2015, Art. no. 651438, doi: 10.1155/2015/651438.
[71] T. Mangel, O. Klemp, and H. Hartenstein, "A validated 5.9 GHz non-line-of-sight path-loss and fading model for inter-vehicle communication," in *Proc. IEEE Conf. Telecommun. (ITST)*, 2011, pp. 75–80.
[72] H. M. El-Sallabi, "Fast path loss prediction by using virtual source technique for urban microcells," in *Proc. IEEE Veh. Technol. Conf.*, vol. 3, 2000, pp. 2183–2187.
[73] D. Cottingham. (2018). *How Wide Are Roads?*. Accessed: Aug. 19, 2018. [Online]. Available: https://mocktheorytest.com/resources/how-wide-are-roads/
[74] W. Yang *et al.*, "Narrowband wireless access for low-power massive Internet of Things: A bandwidth perspective," *IEEE Wireless Commun.*, vol. 24, no. 3, pp. 138–145, Jun. 2017.
[75] Y. Zhuang, J. Pan, and L. Cai, "Minimizing energy consumption with probabilistic distance models in wireless sensor networks," in *Proc. IEEE INFOCOM*, San Diego, CA, USA, 2010, pp. 1–9.
[76] J. K. Young. (2008). *A Practical Guide to Battery Technologies for Wireless Sensor Networking*. Accessed: Jun. 18, 2018. [Online]. Available: https://www.sensorsmag.com/components/a-practical-guide-to-battery-technologies-for-wireless-sensor-networking

Authors' photographs and biographies not available at the time of publication.